Journal of Magnetism and Magnetic Materials 431 (2017) 79–83

Contents lists available at ScienceDirect

Journal of Magnetism and Magnetic Materials

journal homepage: www.elsevier.com/locate/jmmm

Exceptionally large magneto-optical response in dispersions of plate-like nanocrystallites and magnetic nanoparticles

Kathrin May [a,*], Alexey Eremin [a], Ralf Stannarius [a], Balázs Szabó [b], Tamás Börzsönyi [b], Ingo Appel [c], Silke Behrens [c], Susanne Klein [d]

[a] Institut für Experimentelle Physik, Otto-von-Guericke Universität Magdeburg, Universitätplatz 2, 39106 Magdeburg, Germany
[b] Institute for Solid State Physics and Optics, Wigner Research Center for Physics, Hungarian Academy of Sciences, P.O. Box 49, H-1525 Budapest, Hungary
[c] Institut für Katalyseforschung und -technologie; Karlsruher Institut für Technologie (KIT), Postfach 3640, 76021 Karlsruhe; Anorganisch-Chemisches Institut, Ruprecht-Karls Universität Heidelberg, Im Neuenheimer Feld 270, 69120 Heidelberg, Germany
[d] Hewlett-Packard Labs, Long Down Avenue, Stoke Gifford, Bristol BS34 8QZ, UK

ARTICLE INFO

Article history:
Received 11 July 2016
Accepted 26 July 2016
Available online 2 August 2016

ABSTRACT

We introduce a binary colloidal system with an exceptionally strong magneto-optical response. Its induced optical birefringence at even low magnetic fields (in the mT range) reaches a value with the same order of magnitude as that of nematic liquid crystals. This system is based on a binary mixture of plate-like, non-magnetic pigment nanoparticles and a small volume fraction (<1v%) of spherical magnetic nanoparticles. In the field-free state, the suspension is isotropic. Birefringence is caused by an alignment of the pigment platelets, commanded by shape-anisotropic agglomerates of the magnetic nanoparticles in an external magnetic field. We give a semiquantitative discussion about this.

Colloidal suspensions of anisometric (shape-anisotropic) particles exhibit a variety of unique properties, depending on particle concentrations and on external electric fields. Among those are the formation of ordered phases, reversible phase separations, electro-optical switching, and non-linear rheology. Electro- and magneto-optical properties are of particular interest because of potential applications in electrophoretic ink displays, magneto-optical switches and other technologies. There has been a long history of attempts to combine optical properties of molecular liquid crystals (LC) with magnetic properties of ferrofluids by doping nematic phases, following an idea of Brochard and de Gennes [1]. For a long time, these were only partially successful (e.g. [2–4]): The nature of the nematic mesophase often leads to a segregation of the magnetic dopants and degradation of the samples, stability of the suspensions is the main problem. Polymer and elastomer LC doped with ferroparticles are an alternative [5]. Recently, it was shown that suspensions of nano-platelets in nematic liquid crystals can even produce weakly ferromagnetic fluids [6–12].

Here, we use a different strategy and replace the molecular mesogens by suspensions of shape-anisotropic crystals in a non-polar solvent. Lyotropic LC phases formed by dispersed shape-anisotropic particles have been extensively studied in various colloidal systems such as goethite suspensions, fd- and tobacco-mosaic viruses, or clays [13–17]. The existence of ordered phases above critical particle concentrations was predicted by Onsager in the late forties [18]. Inks of elongated pigment needles (Novoperm Carmine) exhibit such a nematic phase already at concentrations as low as 12 v%, and even at lower concentrations, in the isotropic state, these suspensions show an enhanced optical response to external electric fields [19,20]. These pure pigment suspensions do not show appreciable magnetically-induced birefringence in weak (mT) fields. The diamagnetic needles align perpendicular to an external magnetic field at very high field strengths (15–20 T).

In order to achieve an appreciable magneto-optical response at mT fields, one can dope such suspensions with magnetic nanoparticles (MNP). Suspensions of magnetic Fe_3O_4 particles with shape-anisotropic V_2O_5 crystals were shown to exhibit a command effect that can be exploited in magneto-optic switching by Slyusarenko and Kredentser et al. [21,22]. They demonstrated that the orientation of the dispersed magnetic nanorods is transferred by sterical interactions to the non-magnetic component of the mixture. They also described this effect using an Onsager-type theory of binary mixtures [23]. This effect was investigated quantitatively in dispersions of magnetically doped suspensions of V_2O_5 needles [22], where the magnetically induced birefringence reached $1.2 \cdot 10^{-4}$.

In the present study, we dope platelet-like non-magnetic nanocrystals with MNP. Even though the individual MNP are spherical, they form anisometric aggregates in magnetic fields, that are able to command the alignment of the much larger crystallites [24]. We will demonstrate here that this effect is even more

* Corresponding author.

http://dx.doi.org/10.1016/j.jmmm.2016.07.053
0304-8853/

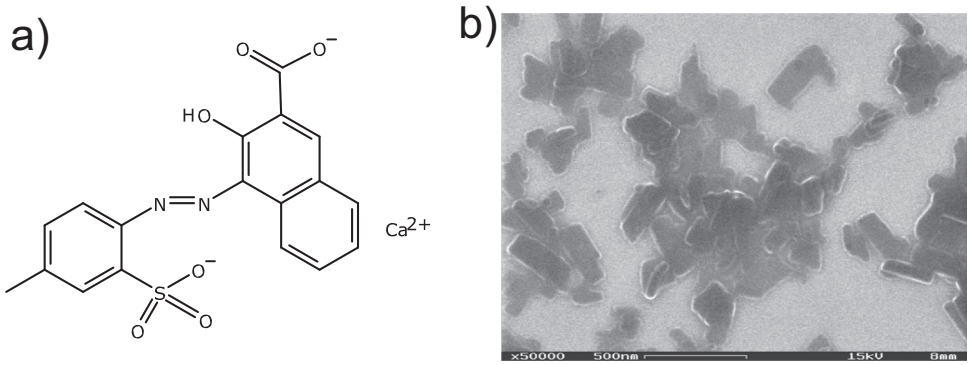

Fig. 1. (a) Chemical formula of a C.I. Pigment Red 176, (b) Scanning electron microscopy (SEM) image of the pigment particles Permanent Rubine, image size 2.3 μm × 1.7 μm.

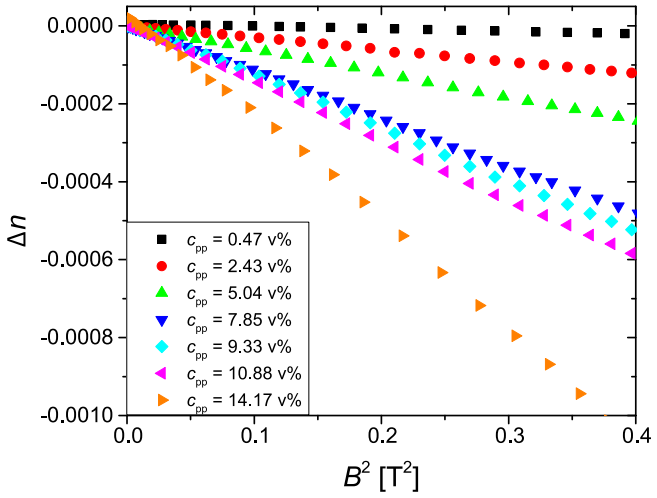

Fig. 2. Magnetically induced birefringence in dispersions of Permanent Rubine in dodecane at various volume fractions.

pronounced for diamagnetic platelet-shaped pigment particles, where the orientation of the platelets in the magnetic field changes with the presence of magnetic particles. The induced optical anisotropy exceeds the Cotton–Mouton-effect of conventional materials by orders of magnitude.

The material used here is Pigment Red 57:1 in its commercially available form *Permanent Rubine L4B01* (*Clariant*, Frankfurt/M, used as received). It is a yellow shade Calcium laked BONS Red pigment. The molecular structure formula of the pigment is shown in Fig. 1a. The primary particles are platelets with an average length of 180 nm ± 81 nm, average width of 64 nm ± 22 nm and an average thickness of 12 nm ± 8 nm [25] (Fig. 1b).

Pigment particles were suspended in the nonpolar solvent dodecane (*Sigma-Aldrich*, Hamburg, used as received) with a commercially available dispersant Solsperse 11200 (*Lubrizol*, Brussels, used as received). Initially, suspensions with pigment concentrations of 20 wt% and above were prepared by milling with the addition of the stabilizer (150 wt% of Solsperse per weight of the pigment). The mixture was milled in a planetary mill (Fritsch Pulverisette 7 premium line), using 0.3 mm yttria stabilized zirconia beads in zirconia lined pots (total 60 min at 500 rpm). Appropriate cooling cycles prevented the temperature inside the pots from rising above 60 °C. Concentrations below 20 wt% were made by stepwise dilution of the base suspension. To test the stability of the suspensions, samples were centrifuged at 10,000 rpm for 60 min. None of the concentrations showed any phase separation into particle-rich and particle-poor zones. Samples left untouched for 12 months did not show any phase separation or aggregation. The suspensions were doped with a commercially available ferrofluid (*Ferrotec*, APG 935). This ferrofluid contains spherical magnetite particles with the diameter of about 10 nm, suspended in hydrocarbons. The surfactant layer thickness is estimated to be about 2 nm. In order to get homogenous mixtures, 3 cycles of about 3 min each in an ultrasonic bath were performed. Dilution for different concentrations of particles was done with dodecane.

Birefringence was measured in sandwich ITO cells (*E.H.C.* and *Instec*) of thicknesses 10 μm or 5 μm. We used the Voigt geometry in which the light direction is perpendicular to the magnetic field, and the polariser and analyzer is oriented at ±45° (to the field direction), respectively. In this geometry, we employed a well-established photoelastic modulator technique [26–28] to measure the optical anisotropy (birefringence Δn). The modulator introduces a time-dependent optical phase shift $\phi(t) = A\sin(\omega t)$. The transmitted light intensity was recorded using a photodetector with the signal measured by a lock-in amplifier. Two Fourier amplitudes of the time dependent photodetector signal are recorded, V_ω and $V_{2\omega}$. The value of the birefringence is given by

$$\Delta n = \frac{\lambda}{2\pi d}\arctan\left(\frac{V_\omega}{V_{2\omega}}\frac{J_2(A)}{J_1(A)}\right),$$

where $\lambda = 632.8$ nm is the laser wavelength and d is the cell thickness. $J_n(A)$ are the Bessel functions of the first kind of integer order n.

Pure dispersions of the Permanent Rubin show a negative birefringence in a magnetic field [29]. This is shown in Fig. 2. The pigment particles behave diamagnetically and appear to have a negative magnetic anisotropy.

The Cotton–Mouton constant calculated from linear fits of the field dependent birefringence is shown in Fig. 3.

The ferrofluid diluted with dodecane also shows very low field-induced birefringence (see Fig. 4). Since the MNP particles are spherically shaped, the birefringence can be attributed to the

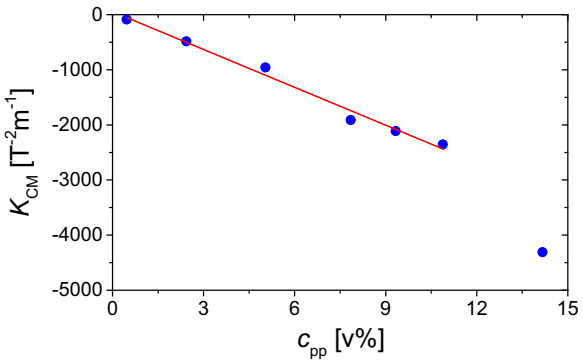

Fig. 3. Cotton–Mouton constant of Permanent Rubine in dodecane at various volume fractions.

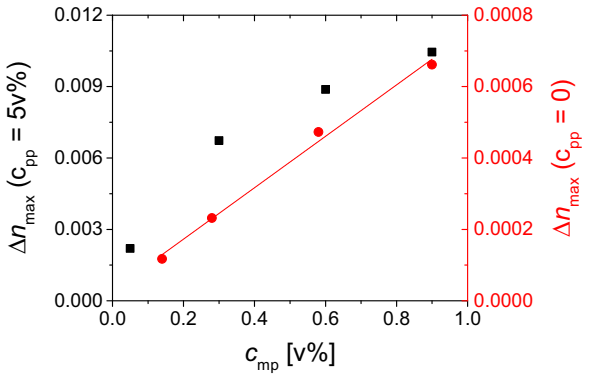

Fig. 4. Magnetically induced birefringence as a function of MNP in a ferrofluid diluted with dodecane (left axis) and of doped Permanent Rubine in dodecane (right axis) at pigment particle concentration c_{pp} = 5 v%.

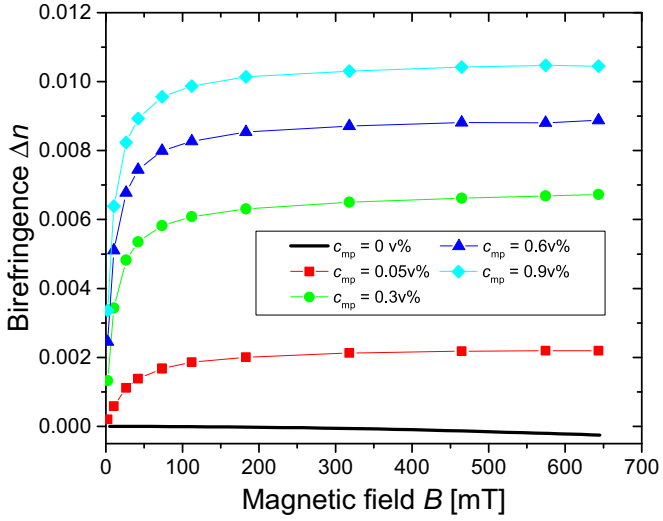

Fig. 5. Birefringence of doped Permanent Rubine in dodecane at pigment particle concentration c_{pp} = 5 v%.

formation of anisometric structures, such as short chains, and their alignment in the magnetic field. The field-induced birefringence of magnetic chains can be described by the model proposed by Xu et al. [30]:

$$\Delta n = 0.5 \cdot n_r \cdot c \cdot g \cdot \left(1 - \frac{3 \cdot \coth(a \cdot B)}{a \cdot B} + \frac{3}{(a \cdot B)^2} \right) \quad (1)$$

where n_r is the refractive index, c is the volume fraction of MNP, $g = \chi_{\parallel} - \chi_{\perp}$ is the anisotropy of the magnetic susceptibility, B is the magnetic field and $a = m_{ch}/(kT)$, where m_{ch} is the magnetic moment of a chain/cluster, k is Boltzmann's constant. Fitting the experimental data with Eq. (1), we obtain the mean magnetic moment of a chain $m_{ch} \approx 5 \cdot 10^{-19}$ Am^2 and $g \approx 0.1$, independent of the concentration. Since the magnetic moment of a single magnetite particle of size 10 nm is $m = 2.34 \cdot 10^{-19}$ Am^2, the mean chain length is estimated to be only slightly more than 2 particles. Surprisingly, the chain length estimated in that way does not depend on the concentration. A reason for this could be that at high concentrations the function in Eq. (1) does not describe satisfactorily the experimental data any more.

Doping Permanent Rubine suspensions with MNP even at small volume fractions drastically enhances the field-induced birefringence, as it is seen in Fig. 5. However, the birefringence of the platelet suspension (c_{pp} = 5 v%) as a function of the concentration

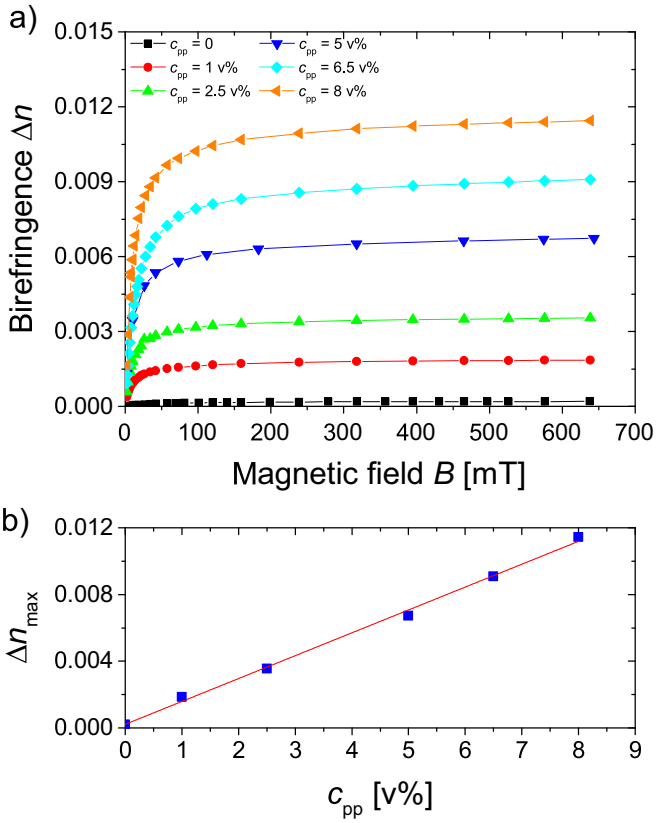

Fig. 6. Magnetically induced birefringence as a function of pigment particles of doped Permanent Rubine in dodecane at MNP concentration c_{mp} = 0.3 v%, (a) dependence on magnetic field, (b) maximum birefringence.

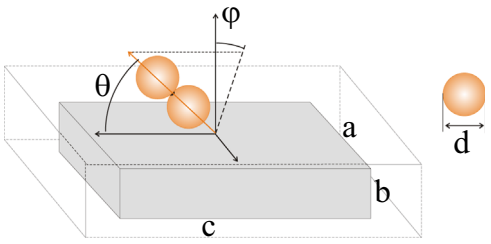

Fig. 7. Sketch of a non-magnetic cuboid platelet (grey) with dimensions $a \times b \times c$ and MNP of diameter d. The volume excluded for the center of mass of the MNP chain is indicated by dashed lines. Angles θ and φ define the orientations of the MNP chain respective to the platelet. We define $b \le a < c$.

of MNP increases slower than a linear function (Fig. 4), in contrast to the rod-like particles Novoperm Carmine [24].

Varying the pigment particle concentration at c_{mp} = 0.3 v%, the maximum birefringence grows linear with the concentration (Fig. 6).

This saturation birefringence Δn_s reaching up to 0.01 is significantly higher than in the other colloidal systems such as clays (e. g. [31]). In contrast to pure dispersions, the slow optical axis aligns parallel to the magnetic field direction. This indicates that the shape anisotropy of the particles is responsible for the field-induced alignment. This effect takes place at a volume fraction of the pigment particles corresponding to the isotropic state. The alignment occurs in the nematic phase too. In this case the director follows an applied magnetic field orienting the MNP.

The origin of the strong magneto-optical response of the pigment/MNP dispersions is the orientation transfer from the magnetic component (MNP) to the non-magnetic one (pigment

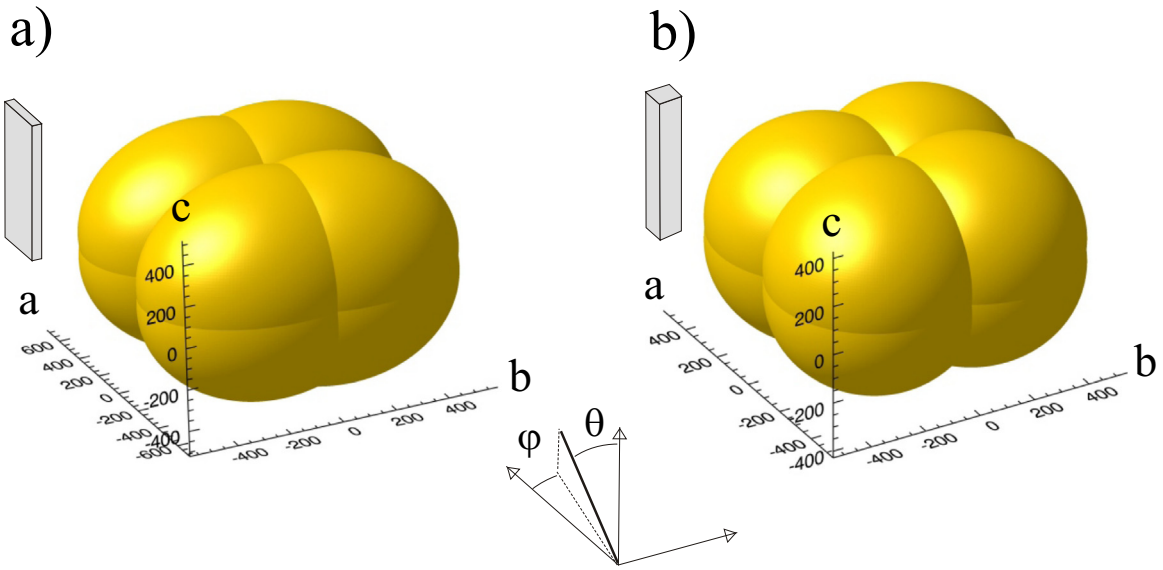

Fig. 8. Dependence of the excluded volume V_{ex} (in units of 10^3 nm^3) on the orientation of the MNP chain (m = 1, d = 14 nm) respective to the cuboid axes, (a) a=64 nm, b=12 nm, c=180 nm, (b) a = b = 27.7 nm, c=180 nm.

platelet particles) and enhanced optical properties of pigments. These properties are material-depended, such as birefringence of the crystalline material, and shape depended, such as shape-anisotropy of absorption. Strong absorption is a particular feature of pigments. These lots of parameters make it difficult to directly compare the platelet particles to the rod-shaped ones. The orientation transfer occurs via steric interactions as the translational entropy of the platelets increases at the cost of the orienational one when the particles align. One important factor describing the efficiency of this process is the relative change of the excluded volume for the particles aligned parallel vs. perpendicular to the MNP chains. When one compares particles of the same material and same volume, platelets have an advantage over the rod-shaped ones as can be shown in a simple calculation below. The idea behind our model is that hard interactions occur when the MNP contact the surface of the considerably larger plate-shaped crystallites. Compared to rod-shaped crystallites of similar volume, the surface of nanoplatelets is much larger and therefore the interactions are stronger. We can formulate a semi-quantitative description on the basis of the excluded volume effect [18]. The alignment transfer from the magnetic dopants to the platelets is a consequence of the reduction of an excluded volume, i.e. the gain of translational entropy, by orientational alignment. Fig. 7 illustrates schematically the geometrical interactions between a platelet and an MNP chain, where we assume a short chain consisting of only two links. Depending on the mutual orientations θ, φ of the partners, a certain volume V_{ex} is excluded for the MNP chain center of mass (sketched by a dashed line). We can estimate this volume by

$$V_e = (a + d + md|\sin\theta\sin\varphi|)\cdot(b + d + md|\sin\theta\cos\varphi|) \cdot(c + d + md|\cos\theta|) \quad (2)$$

where $m + 1$ is the number of MNP in the chain. This equation overestimates the small rounded zones along the edges of the cuboid, but these contribute only by few percent to the excluded volume. If the shortest edge of the platelet b is much smaller than the others (and comparable to d), an orientation of the MNP chain along b increases the excluded volume considerably. For a rod like nanoparticle or a cuboid with a=b, the dependence of V_{ex} on θ and φ is much less pronounced. Fig. 8 visualizes $V_{ex}(\theta, \varphi)$ for two exemplary particle shapes. For the material used here (a) and the shortest possible chain length m=1, the volumes for chain orientations along the three edges a, b, c are 464, 605, and 422 (in 10^3 nm^3), resp., they relate as 1.1: 1.43: 1, the largest and smallest values differ by 43%. For a cuboid with same volume but square cross section, the ratios are 1.24: 1.24: 1, the difference is only 24%. This is reflected in the shapes of the surfaces in Fig. 8. For nanocylinders, the ratio is even closer to unity.

Longer MNP chains create much larger anisotropies. When m=2 the excluded volume variations are 81% for the platelets, but only 46% for rod-like particles. The consequence is a strong tendency for the platelets to align their shortest edges b perpendicular to the MNP chains ($\varphi = \pi/2$) and thus perpendicular to the magnetic field. By that alignment, the excluded volume is minimized and the translational entropy is correspondingly maximized. Respective to the MNP chain orientation (magnetic field direction), the orientational distribution is axially symmetric, the distribution of the flat sides of the platelets is azimuthally uniform. This results in an induced uniaxial birefringence of the suspensions, with the slow axis parallel to the magnetic field. Since the reduction of excluded volume by this alignment is much stronger for platelets, we assume that they are favorable over needles of the same material when one intends to maximize magnetically induced anisotropies.

In summary, we demonstrated in experiments an unusually strong magneto-optic response in a dispersion of elongated plate-shaped pigment particles doped with a small amount (up to 0.17 v%) of ferromagnetic nanoparticles. This response is driven by a steric alignment transfer from the magnetic subphase to the non-magnetic platelets.

Acknowledgments

Financial support by the German Science Foundation (DFG) (Priority Program SPP1681, projects STA 425/36 and BE 2243/2), and the COST Action IC1208 is gratefully acknowledged.

References

[1] F. Brochard, P.G. de Gennes, J. Phys. 31 (1970) 47.
[2] J. Rault, P.E. Cladis, J.P. Burger, Phys. Lett. A 32 (1970) 199.

[3] S.-H. Chen, N.M. Amer, Phys. Rev. Lett. 51 (1983) 2298.
[4] A.M.F. Neto, M.M.F. Saba, Phys. Rev. A 34 (1986) 3483.
[5] L. Zadoina, et al., J. Mater. Chem. 19 (2009) 8075.
[6] A. Mertelj, D. Lisjak, M. Drofenik, M. Copic, Nature 504 (2013) 237.
[7] R. Sahoo, et al., Appl. Phys. Lett. 106 (2015) 161905.
[8] A.J. Hess, Q. Liu, I.I. Smalyukh, Appl. Phys. Lett. 107 (2015) 071906.
[9] O. Riou, et al., Angew. Chem. – Int. Ed. 54 (2015) 10811.
[10] P.M. Rupnik, D. Lisjak, M. Copic, A. Mertelj, Liq. Cryst. 42 (2015) 1684.
[11] N. Dalir, S. Javadian, A.G. Gilani, J. Mol. Liq. 209 (2015) 336.
[12] M. Shuai, et al., Nat. Commun. 7 (2016) 10394.
[13] S. Fraden, G. Maret, D.L.D. Caspar, R.B. Meyer, Phys. Rev. Lett. 63 (1989) 2068.
[14] Z. Dogic, S. Fraden, Phys. Rev. Lett. 78 (1997) 2417.
[15] Z. Dogic, S. Fraden, Langmuir 16 (2000) 7820.
[16] Z. Dogic, A.P. Philipse, S. Fraden, J.K.G. Dhont, J. Chem. Phys. 113 (2000) 8368.
[17] Z.X. Zhang, J.S. van Duijneveldt, J. Chem. Phys. 124 (2006) 154910.
[18] L. Onsager, Ann. N. Y. Acad. Sci. 51 (1949) 627.
[19] A. Eremin, et al., Adv. Funct. Mater. 21 (2011) 556.
[20] K. May, R. Stannarius, S. Klein, A. Eremin, Langmuir 30 (2014) 7070.
[21] K. Slyusarenko, V. Reshetnyak, Y. Reznikov, Philos. Trans. R. Soc. Lond. A 371 (2013) 20120250.
[22] S. Kredentser, et al., Soft Matter 9 (2013) 5061.
[23] H.N.W. Lekkerkerker, P. Coulon, R. Van Der Haegen, R. Deblieck, J. Chem. Phys. 80 (1984) 3427.
[24] K. May, et al., Langmuir 32 (2016) 5085.
[25] R.J. Greasty, et al., Philos. Trans. R. Soc. A 371 (2013) 20120257.
[26] J.C. Kemp, J. Opt. Soc. Am. 59 (1969) 950.
[27] K.W. Hipps, G.A. Crosby, J. Phys. Chem. 83 (1979) 555.
[28] B. Wang, T.C. Oakberg, Rev. Sci. Instrum. 70 (1999) 3847.
[29] Y. Geng, et al., Magneto-optical behaviour of anisometric dispersions in a strong magnetic field, 2016.
[30] M. Xu, P.J. Ridler, J. Appl. Phys. 82 (1997) 326.
[31] D. van der Beek, et al., Phys. Rev. E 73 (2006) 041402.